

# HIGH-GAIN ADVANCED GPS RECEIVER FOR PRECISION GPS APPLICATIONS

Alison Brown, Randy Silva, *NAVSYS Corporation* and Ed Powers, *US Naval Observatory*

## BIOGRAPHY

Alison Brown is the President and CEO of NAVSYS Corp. She has a PhD in Mechanics, Aerospace, and Nuclear Engineering from UCLA, an MS in Aeronautics and Astronautics from MIT, and an MA in Engineering from Cambridge Univ. In 1986 she founded NAVSYS. Currently she is a member of the GPS-III Independent Review Team and Science Advisory Board for the USAF and serves on the GPS World editorial advisory board.

Randy Silva is the lead software architect at NAVSYS Corporation for our integrated GPS products. He has experience developing real-time and Windows-based applications and has over eight years experience with GPS navigation systems. Mr. Silva received his Bachelors Degree from the University of Colorado at Boulder.

Edward Powers is employed as an electronic engineer working in the Time Transfer section of the United States Naval Observatory (USNO) in Washington DC. Previously he worked with the Naval Research Laboratory (NRL) conducting research on various projects related to precise time keeping and GPS satellite clock development. He received both his BS and MS in Engineering from the University of Arkansas (84, 87).

## ABSTRACT

NAVSYS has developed a GPS receiver, the HAGR (High-gain Advanced GPS Receiver), which uses digital beam steering to increase the precision of the GPS observations. In this paper, the HAGR is described and test data is included showing its enhanced performance for high accuracy scientific applications.

When operating in a differential or kinematic positioning mode, HAGR provides low noise observations of the pseudo-range and carrier-phase data. By coherently combining signals from as many as 16 antenna elements, the gain to each satellite tracked can be increased by over 10 dB. Moreover, the digital beam steering approach used also acts to reduce the errors contributed by multipath effects. Test data is presented on the HAGR measurement accuracy for high accuracy scientific applications.

In this paper, the GPS carrier-phase time transfer technique is described and a discussion is included on the error components that currently limit the time-transfer accuracy using this method. Sub-nanosecond time transfer capabilities are expected using GPS carrier-phase observations. Testing to date has shown that conventional GPS receivers introduce significant time offsets in the carrier phase. These offsets are on the order of 1-2 nanoseconds and currently dominate the error budget when performing carrier-phase time transfer. Test data is also presented from the HAGR showing the accuracy of the code and carrier phase observations for time transfer applications.

Report Documentation Page				Form Approved OMB No. 0704-0188	
Public reporting burden for the collection of information is estimated to average 1 hour per response, including the time for reviewing instructions, searching existing data sources, gathering and maintaining the data needed, and completing and reviewing the collection of information. Send comments regarding this burden estimate or any other aspect of this collection of information, including suggestions for reducing this burden, to Washington Headquarters Services, Directorate for Information Operations and Reports, 1215 Jefferson Davis Highway, Suite 1204, Arlington VA 22202-4302. Respondents should be aware that notwithstanding any other provision of law, no person shall be subject to a penalty for failing to comply with a collection of information if it does not display a currently valid OMB control number.					
1. REPORT DATE <b>MAY 2000</b>		2. REPORT TYPE		3. DATES COVERED <b>00-00-2000 to 00-00-2000</b>	
4. TITLE AND SUBTITLE <b>High-Gain Advanced GPS Receiver for Precision GPS Applications</b>				5a. CONTRACT NUMBER	
				5b. GRANT NUMBER	
				5c. PROGRAM ELEMENT NUMBER	
6. AUTHOR(S)				5d. PROJECT NUMBER	
				5e. TASK NUMBER	
				5f. WORK UNIT NUMBER	
7. PERFORMING ORGANIZATION NAME(S) AND ADDRESS(ES) <b>U.S. Naval Observatory, 3450 Massachusetts Avenue, NW, Washington, DC, 20392-5420</b>				8. PERFORMING ORGANIZATION REPORT NUMBER	
9. SPONSORING/MONITORING AGENCY NAME(S) AND ADDRESS(ES)				10. SPONSOR/MONITOR'S ACRONYM(S)	
				11. SPONSOR/MONITOR'S REPORT NUMBER(S)	
12. DISTRIBUTION/AVAILABILITY STATEMENT <b>Approved for public release; distribution unlimited</b>					
13. SUPPLEMENTARY NOTES <b>GNSS 2000, Edinburgh, Scotland, May 2000</b>					
14. ABSTRACT <b>NAVSYS has developed a GPS receiver, the HAGR (High-gain Advanced GPS Receiver), which uses digital beam steering to increase the precision of the GPS observations. In this paper, the HAGR is described and test data is included showing its enhanced performance for high accuracy scientific applications. When operating in a differential or kinematic positioning mode, HAGR provides low noise observations of the pseudo-range and carrier-phase data. By coherently combining signals from as many as 16 antenna elements, the gain to each satellite tracked can be increased by over 10 dB. Moreover, the digital beam steering approach used also acts to reduce the errors contributed by multipath effects. Test data is presented on the HAGR measurement accuracy for high accuracy scientific applications. In this paper, the GPS carrier-phase time transfer technique is described and a discussion is included on the error components that currently limit the time-transfer accuracy using this method. Sub-nanosecond time transfer capabilities are expected using GPS carrier-phase observations. Testing to date has shown that conventional GPS receivers introduce significant time offsets in the carrier phase. These offsets are on the order of 1-2 nanoseconds and currently dominate the error budget when performing carrier-phase time transfer. Test data is also presented from the HAGR showing the accuracy of the code and carrier phase observations for time transfer applications.</b>					
15. SUBJECT TERMS					
16. SECURITY CLASSIFICATION OF:			17. LIMITATION OF ABSTRACT <b>Same as Report (SAR)</b>	18. NUMBER OF PAGES <b>13</b>	19a. NAME OF RESPONSIBLE PERSON
a. REPORT <b>unclassified</b>	b. ABSTRACT <b>unclassified</b>	c. THIS PAGE <b>unclassified</b>			

## INTRODUCTION

The HAGR design is based on NAVSYS' Advanced GPS Receiver (AGR) PC-based digital receiver architecture integrated with a digital beam steering array, see Figure 1<sup>[1]</sup>. Using a proprietary digital signal processing algorithm, the HAGR is able to combine the GPS signals from as many as 16 antennas and create a multi-beam antenna pattern to apply gain to up to eight GPS satellites simultaneously. The HAGR 16-element antenna array is shown in Figure 2. Testing has also been conducted with our miniature antenna array, shown in **Figure 3**<sup>[2,3]</sup>.

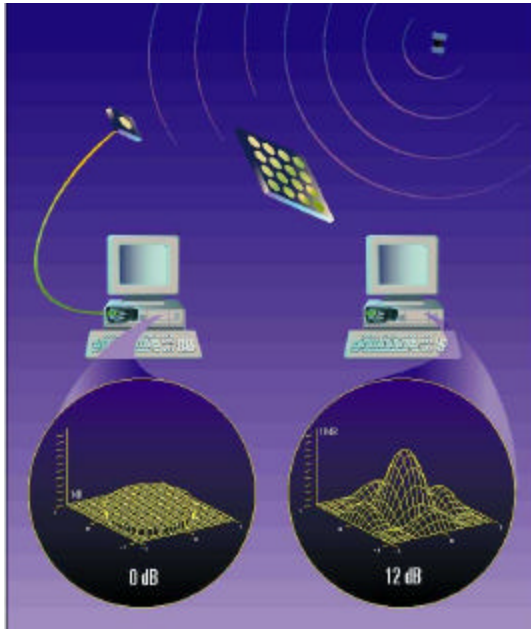


**Figure 1 High-gain Advanced GPS Receiver (HAGR)**

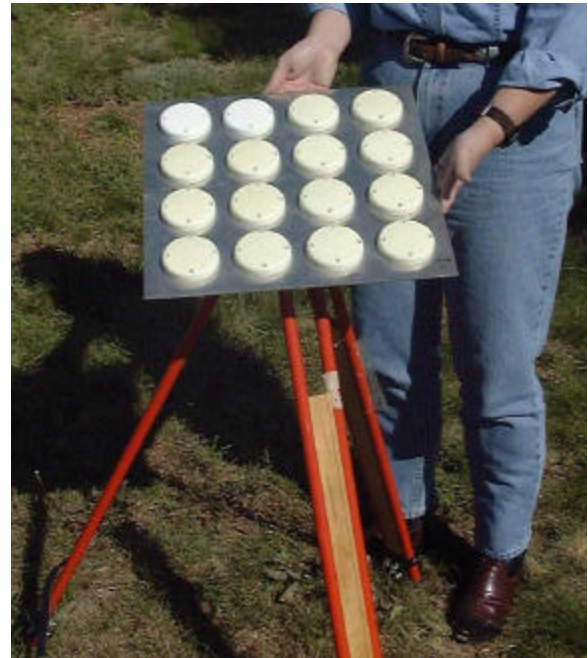


**Figure 2 HAGR 16-element antenna array**

The performance specifications for the HAGR for a 16-element, L1 C/A code version of this product are included in reference<sup>[4]</sup>. Currently an L1/L2 Precise Position System (PPS) version of the HAGR (the HAGR-200) is also in development.

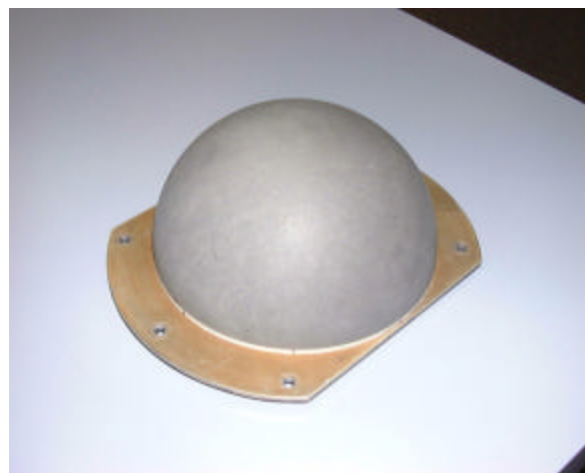


**Figure 3 6" diameter 4-element Mini-Array**

## HAGR SYSTEM ARCHITECTURE

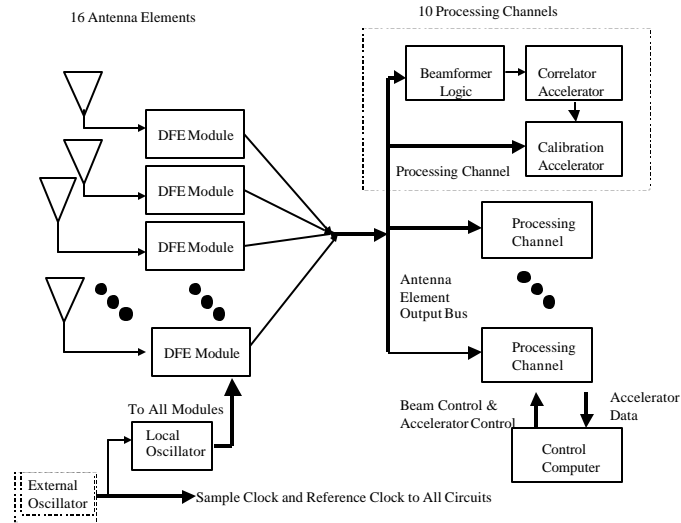


**Figure 4 HAGR System Block Diagram**

The HAGR system architecture is shown in Figure 4. The signal from each antenna element is digitized using a Digital Front-End (DFE). The bank of digital signals is then processed by the HAGR digital-beam-steering card to create a composite digital beam-steered signal input for each of the receiver channels. Figure 5 illustrates the beam-forming satellite geometry and mathematical expression for line of sight (los).

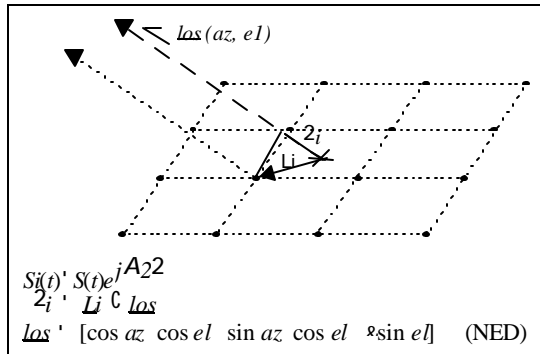


**Figure 5 Beam forming satellite geometry**

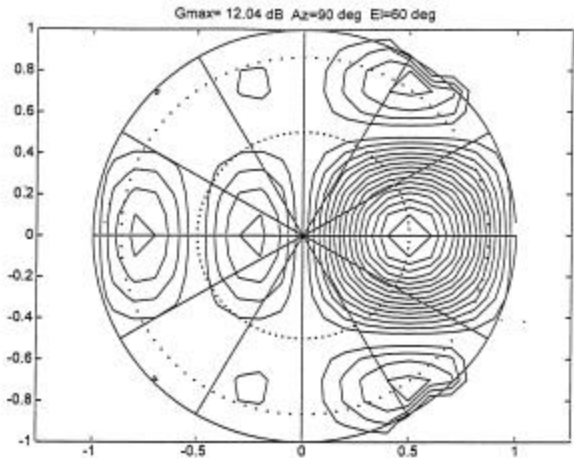


**Figure 6 16-element array composite beam pattern**

If attitude data (pitch, roll, yaw) is provided from an inertial navigation system or attitude sensor, the HAGR will operate while the antenna is in motion<sup>[5]</sup>. The default mode, for static operation, is to align the array pointing north.

The digital beam forming provides significant benefits in improving the measurement accuracy due to the narrow beam antenna pattern directed at each satellite tracked. As shown in Figure 6, a 16-element array will provide up to 12 dB of additional gain on each satellite tracked.

## DGPS AND KGPS NAVIGATION ACCURACY

The accuracy of a differential GPS (DGPS) solution is a function of the solution geometry and the accuracy of the raw pseudo-range measurements as shown in Equation 1 and Equation 2. A similar equation also exists for a Kinematic GPS (KGPS) solution which is derived from carrier phase observations and a solution of the integer carrier cycle ambiguities (see Equation 3).

Equation 1

$$G = (H^T H)^{-1}$$

$$H = \begin{bmatrix} 1_1^T & 1 \\ 1_2^T & 1 \\ \cdot & \cdot \\ \cdot & \cdot \\ 1_n^T & 1 \end{bmatrix}$$

$$PDOP = \sqrt{G_{11} + G_{22} + G_{33}}$$

Equation 2

$$E[\tilde{x}_{DGPS}^T \tilde{x}_{DGPS}] = PDOP^2 \mathbf{s}_{DGPS}^2 \approx PDOP^2 (\mathbf{s}_{PR}^2 + \mathbf{s}_{Mpr}^2)$$

Equation 3

$$E[\tilde{x}_{KGPS}^T \tilde{x}_{KGPS}] = PDOP^2 \mathbf{s}_{KGPS}^2 \approx PDOP^2 (\mathbf{s}_{cph}^2 + \mathbf{s}_{Mcph}^2) \mathbf{I}^2$$

The major benefits of the HAGR digital beam forming for DGPS and KGPS navigation applications are the increase in accuracy of the pseudo-range and carrier-phase observations and the reduction in multipath errors due to the antenna directivity. These benefits are discussed in this section.

The differentially corrected pseudo-range accuracy is dominated by two error sources as illustrated in Equation 4. The first is receiver noise and the second is the multipath error. The receiver noise is a function of the effective delay-lock-loop bandwidth after carrier smoothing is applied. This can be computed from the following equation where  $T_C$  is the C/A code chip length (293 meters),  $d$  is the correlator chip spacing and  $C/N_0$  is the received signal-to-noise ratio in dB-Hz.

Equation 4

$$\mathbf{s}_{PR} = T_c \sqrt{\frac{d B_{DLL}}{2 \cdot 10^{C/N_0/10}}} \left( 1 + \frac{2 B_{IF}}{(2-d) 10^{C/N_0/10}} \right)$$

This is plotted in Figure 7 against  $C/N_0$  assuming a 1 Hz bandwidth delayed locked loop (no carrier smoothing), a code chip separation of 1 and an accumulation frequency of 1-kHz.

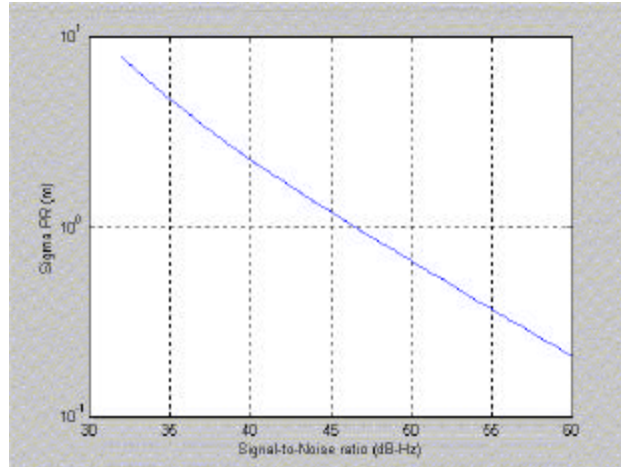


**Figure 7 Sigma PR Noise vs C/N0 (Bd11=1, d=1)**

From Figure 7, a 10 dB increase in signal power will have the affect of reducing the pseudo-range noise by a factor of 0.3. The HAGR routinely receives satellite signals with  $C/N_0$  of 54 to 58 dB-Hz which reduces the pseudo-range noise level to below 10 cm with carrier smoothing.

### HAGR MEASUREMENT ACCURACY

The increase of about 10 dB in signal-to-noise ratio from the HAGR digital beam forming is shown in Figure 8 to Figure 10, compared against two conventional GPS reference receivers<sup>[1]</sup>. From these plots, it can be seen that the HAGR  $C/N_0$  is significantly higher than the reference receiver, demonstrating the effect of the gain from the digital beam forming.

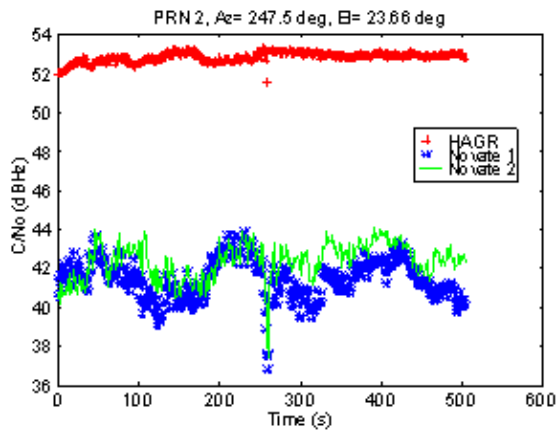


**Figure 8 SNR Comparison Between 16-Antenna HAGR and Novatel's for PRN 2**

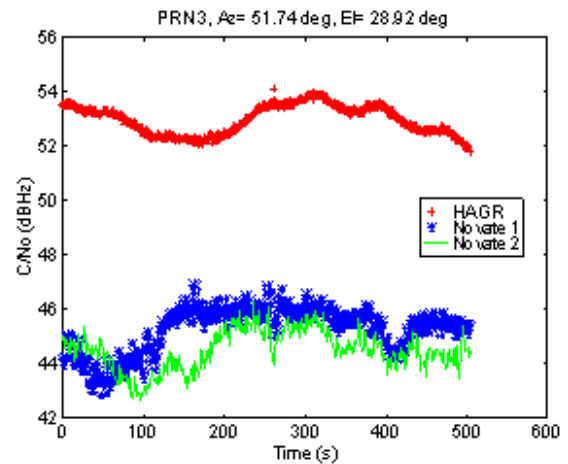


**Figure 9 SNR Comparison Between 16-Antenna HAGR and Novatel's for PRN 3**

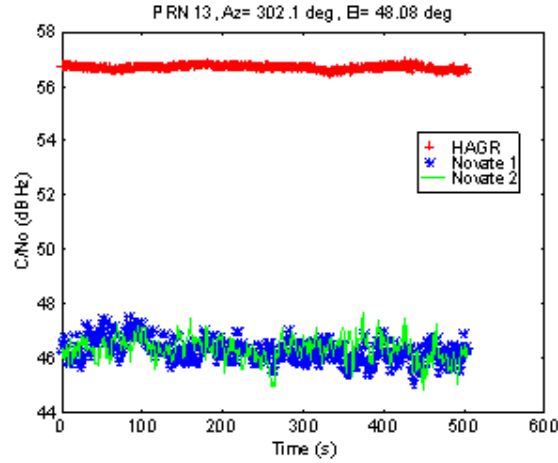


**Figure 10 SNR Comparison Between 16-Antenna HAGR and Novatel's for PRN 13**

The increased gain also results in improved pseudo-range and carrier-phase tracking performance, and the directionality of the beam-steering antenna array reduces the effect of multipath on the solution. In Table 1, the short term noise is listed for each of the two HAGR units tested. The gain provided by the beam steering has maintained the signal-to-noise generally above 50 dB-Hz, providing sub-meter level short term noise on the pseudo-range performance. This increased accuracy reduces the time needed to resolve the carrier-cycle ambiguities needed for computing kinematic position solutions or a carrier-phase time transfer solution.

**Table 1 HAGR PR Noise Performance Data**

SVID	AZ	EL	C/N0 1	$s_{PR}$	C/N0 2	$s_{PR}$
3	285	36	49	0.89	51	0.46
6	173	18	44	0.60	44	0.48
8	134	21	48	0.46	45	1.05
9	90	28	50	0.50	48	0.77
17	113	57	55	0.21	55	0.19
21	291	50	54	0.26	53	0.31
23	21	66	55	0.35	54	0.47
26	43	13	49	0.33	52	0.27
29	212	40	52	0.38	53	0.36

Multipath errors are caused by the receiver tracking a composite of the direct GPS signals and reflected GPS signals from nearby objects. The resulting pseudo-range error and carrier-phase error is a function of the phase offset between the direct and multipath signals and the relative signal strength. For a fixed installation, these errors appear as biases, changing only as the line-of-sight to the satellite changes due to the satellite motion. Multipath mitigation techniques have been developed using multi-correlator techniques that improve the performance of the code tracking loops in the presence of multipath. However, these have little effect against carrier-phase errors introduced by the multipath signals. The HAGR digital beam-former has the advantage that the multipath is reduced on both the pseudo-range and the carrier-phase errors through the directivity of the antenna pattern towards the satellite which reduces the effect of the multipath signal.

The effect of multipath on the GPS signals can be modeled through the following equations.

Equation 5

$$\begin{aligned} s(t) &= AC(t + \mathbf{t}) \sin(\mathbf{w}t + \mathbf{q}) + A_M C(t + \mathbf{t}_M) \sin(\mathbf{w}t + \mathbf{q}_M) \\ s(t)\hat{s}(t) &= AR(\mathbf{t} - \hat{\mathbf{t}}) \sin(\mathbf{w}t + \mathbf{q}) + A_M R(\mathbf{t}_M - \hat{\mathbf{t}}) \sin(\mathbf{w}t + \mathbf{q}_M) \\ &= (A + \tilde{A}) \sin(\mathbf{w}t + \mathbf{q} + \tilde{\mathbf{q}}) \end{aligned}$$

The above equation can be solved for the pseudo-range error that will be observed with the DLL tracking loops and the phase error that will be observed by the PLL tracking loops. This simplifies to the following expression, if it is assumed that the multipath reflections are relatively close to the antenna (compared with the C/A code chip length of 293 m) and that  $R(\tau)$  from the DLL is approximately equal to one for both the direct and multipath signals.

Equation 6

$$\tilde{\mathbf{t}} = \frac{A_M^2}{A^2} \mathbf{t}_M$$

This equation represents the approximate maximum error for a 1-chip Early/Late correlator assuming that the multipath delays are less than 1/2 chip. If the multipath errors are 10 dB down from the satellite signal power, then the multipath error will be approximately 10% of the multipath delay. For example, if signals are received with a delay of 20 meters, then the multipath error will be less than 2 meters on the pseudo-range observation. Since the beam-forming antenna provides 10 dB gain in the direction of the satellite signal, the multipath signals are received with at least 10 dB lower power than the direct satellite signals.

Equation 7

$$\begin{aligned} \tilde{A} / A &= |A + A_M e^{j\Delta q}| / A \\ \tilde{\mathbf{q}} &= \angle(A + A_M e^{j\Delta q}) \\ \Delta \mathbf{q} &= \mathbf{q} - \mathbf{q}_M \end{aligned}$$

In Figure 11 the effect of the multipath signal on the C/N0 envelope is shown as a function of the multipath signal power. In Figure 12 the multipath phase angle errors and signal amplitude are shown versus the multipath phase angle offset ( $\Delta\theta$ ) for the cases when  $A_M=A$  (0 dB),  $A_M=A/\sqrt{2}$  (-3dB down),  $A_M=A/2$  (-6dB down), and  $A_M=A/\sqrt{10}$  (-10 dB down). This figure illustrates the benefit of the beam former in also limiting multipath errors on the phase observations – a key area of concern for kinematic GPS applications.



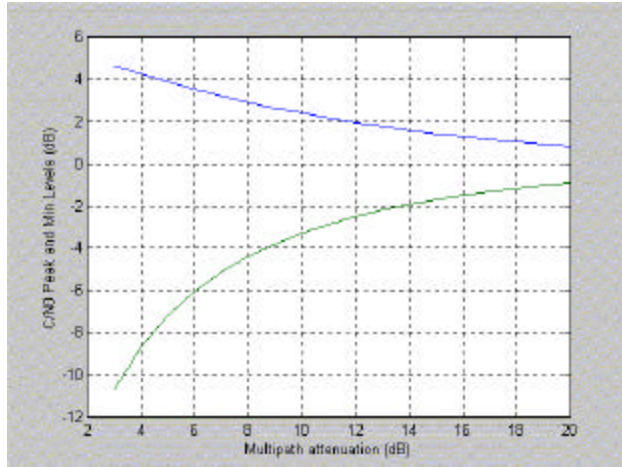


**Figure 11 Multipath Amplitude Effect**

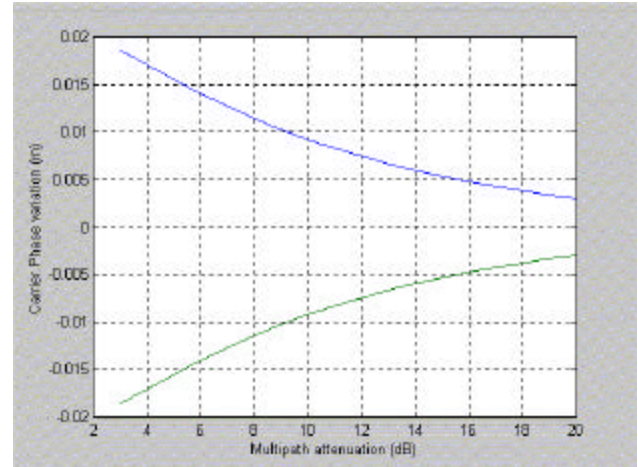


**Figure 12 Multipath Phase Angle Error**

The multipath effect on the GPS measurements is difficult to observe directly. The best indication of the magnitude of multipath errors is from the variation in C/N0 and the short-term difference between PR+CPH which are both dominated by multipath errors. Test data taken with two HAGRs indicated that, with beam-forming, the majority of the satellite signals have an C/N0 delta of less than 2 dB [4]. From Figure 11 and Figure 12, the carrier phase variation would be expected to be less than  $\pm 5$  mm when the multipath signal is below this level.

It should be noted from Figure 12 that a strong multipath signal can cause phase variations on the order of  $\pm 2$  cm which would severely affect the kinematic GPS performance for a single-element GPS receiver. To compare the performance of the antenna array with and without the beam steering, the residual phase error on each of the individual elements of the antenna array is plotted in Figure 13. This shows that the carrier phase error can easily be offset by  $\pm 0.1$  cycles (2 cm) between the individual elements. For high accuracy applications, the multipath rejection from spatial processing the HAGR array signals can significantly reduce this error source.

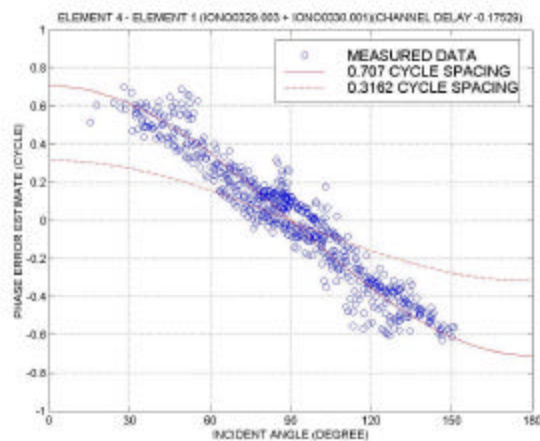


**Figure 13 Carrier-phase multipath without beam steering**

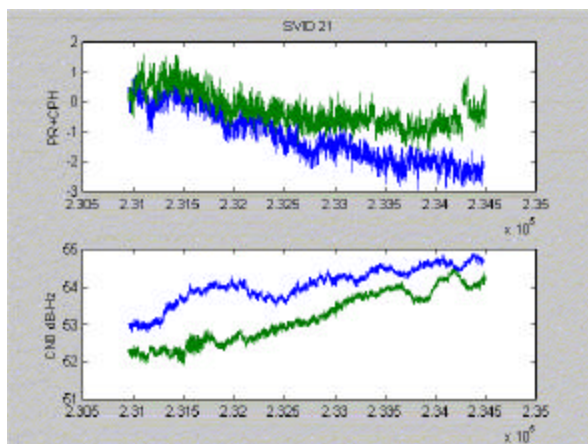


**Figure 14 PR+CPH -SV 21**

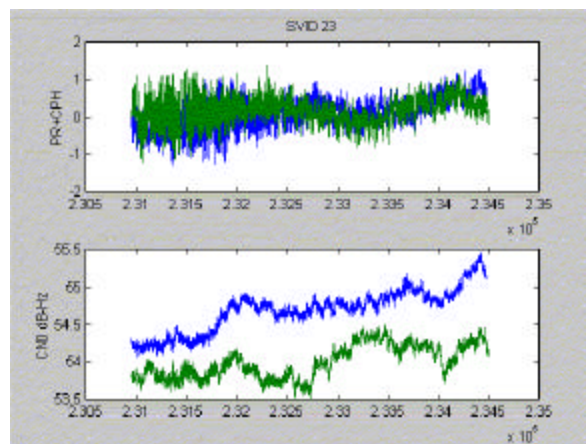


**Figure 15 PR+CPH -SV 23**

## KINEMATIC GPS TEST RESULTS

The kinematic performance of the HAGR antennas was tested by setting each of the antennas on two survey marks. The remote antenna array was located 0.793 meters East of the reference antenna array. The NAVSYS's kinematic GPS software was used to process the data. Figure 16 to Figure 18 show the processing results. During the test, 6 valid satellites were available. These test results show that the kinematic GPS positioning error achieved a standard deviation of 4 mm (1-sigma) in the north and east directions and 6 mm (1-sigma) vertically. This is consistent with a carrier phase measurement accuracy of 3 mm (1-sigma). These test results show that the multipath errors on the carrier phase are maintained on the order of a few millimeters by the HAGR beam forming. The mean offset between the two antennas observed by the kinematic solution was 0.7933 meters which agreed to the surveyed location to within the precision of our measurement capability.

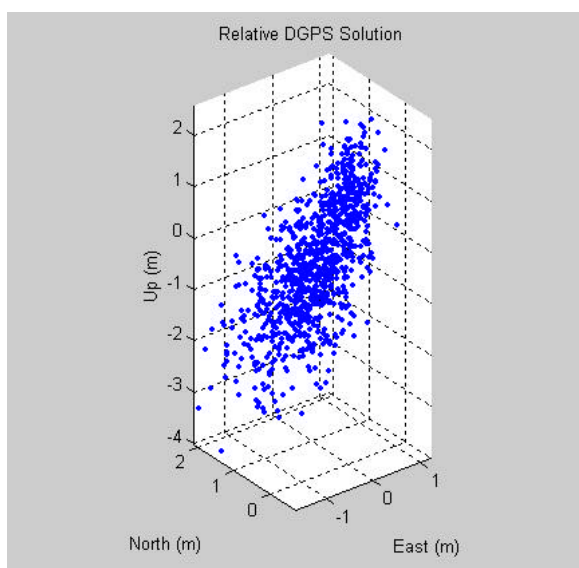


**Figure 16 HAGR DGPS Position Solution**

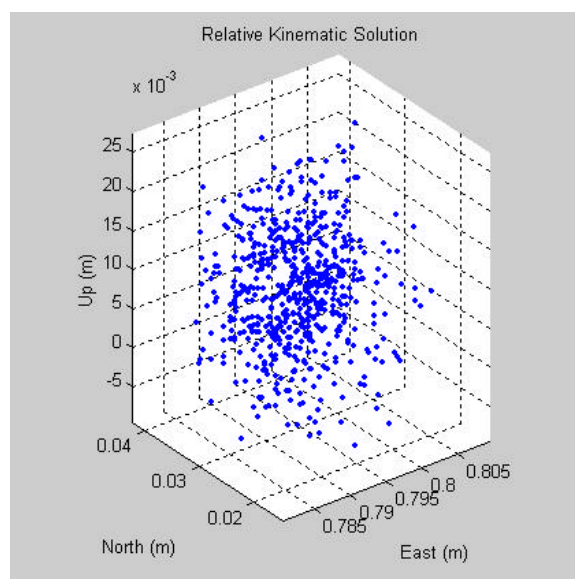


**Figure 17 HAGR KGPS Position Solution**

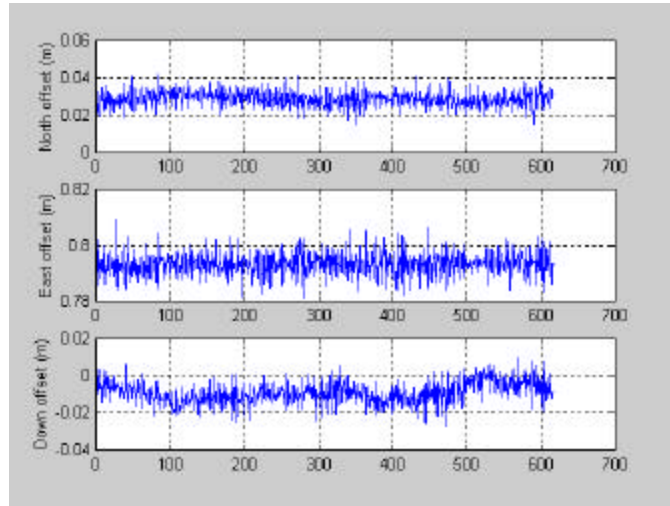


**Figure 18 HAGR Kinematic Position Solution (NED)**

### **GPS CARRIER PHASE TIME TRANSFER**

In this section of the paper, the performance of the HAGR in performing GPS carrier-phase time transfer technique is described. Previous testing with conventional GPS receivers has shown that carrier phase instabilities can cause offsets on the order of 1-2 nanoseconds, which currently dominates the error budget when performing carrier-phase time transfer. The ability of NAVSYS' HAGR to make phase coherent measurements from multiple antenna elements, also means that it provides a highly phase stable observation of the GPS carrier, relative to a local reference oscillator. This allows the HAGR to provide highly precise time observations for carrier-phase time transfer.

GPS carrier-phase measurements provide the potential for much improved precision in time and frequency transfer<sup>[6,7,8]</sup>. Time-Transfer errors approaching 100 picosecond (ps) are expected using this approach. Typical carrier phase measurement noise can be on the order of ten ps whereas the code measurement noise can be as high as ten nanoseconds (ns). Multipath errors are also much smaller on the carrier-phase observations than on the code-based pseudo-range measurements. Accordingly, GPS carrier-phase measurement accuracy is 100 to 1000 times better than the code based pseudo-range measurements.

The GPS system errors that affect the accuracy of the carrier-phase time transfer performance are listed in Table 2

**Table 2 GPS System Errors**

- |  |
|--|
| <ol style="list-style-type: none"> <li>1. Dual Frequency Ionosphere errors (calibration bias, increase noise)</li> <li>2. Troposphere errors (Weather data, Models)</li> <li>3. Receiver Measurement Noise</li> <li>4. Multi-path Noise</li> <li>5. Satellite Position (Orbits)</li> <li>6. Station Position (Location)</li> </ol> |
|--|

Test results have shown that the dominant errors currently affecting the accuracy of carrier-phase time transfer, are not the GPS system errors shown in Table 2, but are due to environmental effects within the GPS receiver.

The time delay of the GPS signal as it propagates through a complete GPS receiving system consists of the delay through the GPS receiver, GPS antenna cables and the GPS antenna with its associated antenna electronics. All of these GPS receiving system sub-components are affected by environmental influences. Studies of the temperature sensitivities of several of these GPS receiving systems have shown delay variations of as great as several nanoseconds per degree C.<sup>[9 10 11]</sup>

**Table 3 GPS Receiver Temperature Sensitivity**

	Temperature effect
Receiver Code Measurements	(150 – 1500) ps per °C
Receiver Carrier Measurements	(10 – 200) ps per °C
Antenna cable	0.5 ps per °C per Meter
Antenna electronics	(5 – 50) ps per °C

Since all of these temperature effects are common to all receiver channels, these errors are mapped into the users local clock error. This does not affect the use of this data for typical geo-location application, but for time transfer applications these temperature effects must be minimized. Specially constructed phase-stabilized antenna cables can be used that will reduce the delay fluctuations through the antenna cable by a factor of 20 or more. However, the GPS receiver front-end itself must also be designed to provide a highly stable carrier-phase reference over temperature variations. This has been accomplished in the HAGR design.

## TIME TRANSFER LAB TEST RESULTS

To test the time transfer performance of the HAGR receiver, two receivers were set up to operate using a common 10 MHz time reference and also a common antenna. This test will cancel the GPS system errors shown in Table 2, leaving the effect of the carrier phase observation and uncalibrated receiver errors on the solution.

The raw carrier phase difference was computed between the two receivers for each satellite tracked. This was corrected for the integer ambiguity offset only. The residual error between two data sets for each satellite is plotted in Figure 19 and Figure 20. The HAGR was power-cycled between these two data sets. As can be seen, both data sets observed a common bias between the units of around 0.02 cycles and has a standard deviation of the carrier-phase difference residual of 16 psecs. Each satellite observes a common offset between the units of 14 psecs +/- 3 psecs, indicating that the HAGR units should be able to be calibrated to this level by averaging the satellite observations.

**Table 4 Carrier-phase time difference accuracy**

SVID	1	14	16	18	22	25
Mean offset (cycles)	0.022	0.020	0.022	0.026	0.022	0.020

Mean offset (psec)	14.3	12.4	14.1	16.8	13.7	12.4
Std Dev (psec)	15.1	17.6	16.3	16.4	15.4	9.2

This testing indicates that the HAGR units can provide carrier phase observations consistent with a time transfer performance of 16 ps 1-sigma, post-calibration. The testing performed using the HAGR highlighted the benefit of a highly stable front-end and also identified key requirements for the LO generation which are being designed into our core product. Testing on these units is continuing to show their phase stability from turn-on to turn-on and also repeating these tests over temperature. Testing is also planned using a dual-frequency (L1/L2) P(Y) code version of the HAGR.

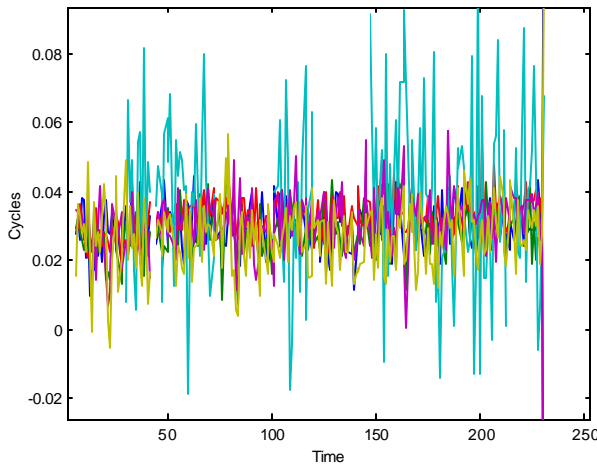


**Figure 19 Unit1-Unit2 Time Offset (cycles) Time Set 1**

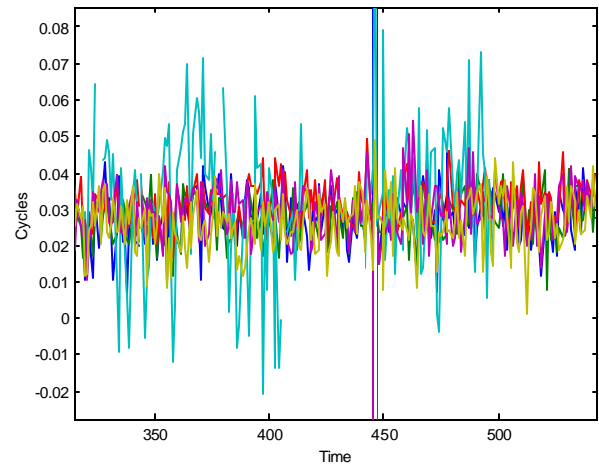


**Figure 20 Unit1-Unit2 Time Offset (cycles) Data Set 4**

## CONCLUSION

In conclusion, the test data taken to date on two single-element HAGR units indicates that the HAGR is capable of making high accuracy pseudo-range and carrier phase observations suitable for precision positioning and timing applications. Test data showed that the pseudo-range accuracy could be maintained at the sub-meter level even before carrier smoothing. This significantly improves the differential accuracy from the HAGR and also speeds the time required to perform carrier cycle ambiguity resolution. The kinematic test data showed that the relative position errors were within 4 mm (horizontal) and 6 mm (vertical) which is consistent with a carrier phase error of around 3mm (1-sigma). This improved accuracy demonstrates the advantage of the HAGR antenna array in reducing multipath errors.

The carrier phase time transfer testing performed showed that the carrier phase random errors (1-Hz) were maintained at around 16 picoseconds (1-sigma). When these errors are smoothed against a precision clock, the time transfer error could be expected to approach the tolerance of the HAGR phase calibration, which is around  $\pm 3$  ps in these tests.

Further improvements in pseudo-range and carrier phase multipath reduction can be achieved by optimizing the HAGR weights to adapt to detected multipath signals. Since the HAGR digital

beam steering is performed under software control, this capability could be added to the current system design. Research is currently being conducted on the performance benefits that can be achieved through an adaptive multipath spatial processing algorithm.

Based on these results, and previous testing of the HAGR<sup>[4]</sup>, this GPS receiver has the following advantages for precision positioning and timing applications.

- Highly stable, phase-coherent front-end, phase-locked to an external 10 MHz oscillator
- Increased C/N0 to the satellite observations using beam-steering
- High accuracy pseudo-range and carrier-phase observations for rapid carrier-cycle ambiguity
- Multipath minimization on both pseudo-range and carrier-phase from the digital beam-steering
- L1/L2 P(Y) code HAGR in development

## ACKNOWLEDGEMENT

This work was performed under contract to the Office of Naval Research (ONR) with funding also provided by the US Naval Observatory.

---

<sup>1</sup> Dr. Alison Brown, Randy Silva, Gengsheng Zhang, "Test Results of a High Gain Advanced GPS Receiver", ION 55<sup>th</sup> Annual Meeting, Cambridge, MA, June 1999

<sup>2</sup> A. Brown, K. Taylor, R. Kurtz and H. Tseng, "Kinematic Test Results Of A Miniaturized GPS Antenna Array With Digital Beamsteering Electronics," ION National Technical Meeting, Anaheim, CA, January 2000

<sup>3</sup> A. Brown, D. Reynolds, and H. Tseng, "Miniaturized GPS Antenna Array and Test Results," Proceedings of GNSS 2000, Edinburgh, Scotland, May 2000.

<sup>4</sup> A. Brown and J. Wang, "High Accuracy Kinematic GPS Performance Using A Digital Beam-Steering Array," Proceedings of ION GPS-99, Nashville, TN, September 1999

<sup>5</sup> A. Brown, H. Tseng, and R. Kurtz, "Test Results of a Digital Beamforming GPS Receiver for Mobile Applications," Proceedings of ION National Technical Meeting, Anaheim, CA, January 2000.

<sup>6</sup> K. Larson and J. Levine, "Carrier-Phase Time Transfer," IEEE Transactions on Ultrasonics, Ferroelectrics, and Frequency Control, VOL. 46, NO. 4, July 1999

<sup>7</sup> G. Petit and C. Thomas "GPS Frequency Transfer using Carrier Phase Measurements," Proceedings of the 1996 IEEE Internal Frequency Control Symposium

<sup>8</sup> D. Jefferson, S. Lichten, and L. Young, "A Test of Precision GPS Clock Synchronization," in Proc. 1996 IEEE Freq. Control Symposium, Honolulu, HI, pp. 1206 – 1210

<sup>9</sup> L. Nelson, K. Larson and J. Levine, "Review of GPS Carrier-Phase and Two-Way Satellite Time Transfer Measurement Results between Schriever Air Force Base and the United States Naval Observatory," Proceedings of ION GPS-99, Nashville, TN, September 1999

<sup>10</sup> F. Overney, Th Schildknecht, G. Beutler, L. Prost and U. Feller, "GPS Time Transfer using Geodetic Receivers: Middle-term Stability and Temperature Dependence of the Signal Delays: Proceedings of the European Frequency and Time Forum," Neuchatel, March 1997

<sup>11</sup> E Powers, P. Wheeler, D. Judge and D. Matsakis, "Hardware Delay Measurements and Sensitivites in Carrier Phase Time Transfer", Proceedings of Precise Time and Time Interval (PTTI) Conference, Reston, VA, December 1998.